REPORT DOCUMENTATION PAGE

Form Approved
OMB NO. 0704-0188

1. AGENCY USE ONLY (Leave Blank)	2. REPORT DATE 11.20/2003 November 2003	3. REPORT TYPE AND DATES COVERED Final report, September 2001 to ~~November~~ 10 9 May 2003

4. TITLE AND SUBTITLE
Incorporation of Amorphous Metals into MEMS for High Performance and Reliability

5. FUNDING NUMBERS
DAAD19-01-C-0084

6. AUTHOR(S)
John R. Porter (Compiler)
Jeffrey DeNatale, Natalie Gluck, Daniel Branagan (INEEL)

7. PERFORMING ORGANIZATION NAME(S) AND ADDRESS(ES)
Rockwell Scientific Company
1049 Camino Dos Rios
Thousand Oaks, CA 91360

8. PERFORMING ORGANIZATION REPORT NUMBER
GO 71189

9. SPONSORING / MONITORING AGENCY NAME(S) AND ADDRESS(ES)
U. S. Army Research Office
P.O. Box 12211
Research Triangle Park, NC 27709-2211

10. SPONSORING / MONITORING AGENCY REPORT NUMBER
42873.1-MS

11. SUPPLEMENTARY NOTES
The views, opinions and/or findings contained in this report are those of the author(s) and should not be construed as an official Department of the Army position, policy or decision, unless so designated by other documentation.

12 a. DISTRIBUTION / AVAILABILITY STATEMENT
Approved for public release; distribution unlimited.

12 b. DISTRIBUTION CODE

13. ABSTRACT (Maximum 200 words)

Amorphous or amorphous derived metals have properties that can be very different from their crystalline counterparts. Since mechanisms for crystalline slip are absent, they can have high hardness and strength and exhibit high elastic strain before failure. Increasing the elastic limit of a component metal has the potential to enable the redesign of MEMS components to achieve higher performance for a given size device. To exploit these properties, Rockwell Scientific teamed with INEEL to develop the MEMS process flow to incorporate amorphous metals into MEMS devices.
This report summarizes the results of a program to investigate one amorphous metal for MEMS insertion. The technologies developed in this program include:

1. Successful preparation of deposition targets by thermal spraying at INEEL.
2. Successful deposition of uniform coatings of amorphous alloy on silicon substrates by both laser ablation and sputtering.
3. Successful processing of MEMS test structures incorporating amorphous metals demonstrating.

Only one amorphous alloy has been investigated and other amorphous alloys may prove more suitable for specific applications. Issues such as residual stress control, material property optimization and property characterization remain in need of further work.

14. SUBJECT TERMS	15. NUMBER OF PAGES
MEMS, amorphous metals, laser ablation	40
	16. PRICE CODE

17. SECURITY CLASSIFICATION OR REPORT	18. SECURITY CLASSIFICATION ON THIS PAGE	19. SECURITY CLASSIFICATION OF ABSTRACT	20. LIMITATION OF ABSTRACT
UNCLASSIFIED	**UNCLASSIFIED**	**UNCLASSIFIED**	**UL**

Incorporation of Amorphous Metals into MEMS for High Performance and Reliability

DARPA Contract No.: DAAD19-01-C-0084

Final Report

November, 2003

Principal Investigators, John R. Porter, 805-373-4702, jporter@rwsc.com
Jeffrey DeNatale, 805-373-4439, jnatale@rwsc.com
Program Manager, John R. Porter, 805-373-4702, jporter@rwsc.com,

Rockwell Scientific Co.
1049 Camino Dos Rios
Thousand Oaks, CA 91360
jporter@rwsc.com

Table of Contents

1.0 Executive Summary

Amorphous or amorphous derived metals have properties that can be very different from their crystalline counterparts. Since mechanisms for crystalline slip are absent, they can have high hardness and strength and exhibit high elastic strain before failure. By precluding mechanisms for plastic deformation, there is also no mechanism for fatigue damage to accumulate. The absence of any grain boundaries eliminates a mechanism for corrosion and amorphous metals have also been reported to have excellent corrosion and wear properties. This combination of properties suggests that the incorporation of amorphous metals into MEMS devices could enable the design of selected MEMS devices with significantly improved performance and reliability.

This report summarizes the results of a seed program to investigate this potential for improved performance of MEMS devices by the incorporation of one representative amorphous metal into their structure. For this, RSC teamed with Idaho National Engineering and Environmental Laboratory (INEEL). Dr. Daniel Branagan of INEEL has developed a family of iron-based amorphous metals as very hard, corrosion resistant coatings for steels. Two of these compositions were selected for investigation in this program. The technologies developed in this program include the following:

1. Successful preparation of targets (for sputtering and laser ablation) of DAR27 by thermal spraying using a high velocity oxyfuel gun (HVOF) at INEEL.
2. Successful coating of ~ 0.5 μm thick, uniform coatings of DAR27 on silicon substrates by both laser ablation and sputtering.
3. Successful processing of MEMS test structures incorporating amorphous metals demonstrating:

   Excellent edge definition using standard photolithography and MEMS processing techniques

   Successful metal lift-off using polyimide, sacrificial layers and standard etching methods.

New alloy development was not a part of this seed program. However, techniques were developed to measure the properties of the amorphous material that would be applicable to other metals that might be developed in a subsequent program. The properties of thin film DAR27 measured in this contract include hardness, modulus, and corrosion resistance. Tribology measurements and strength measurements were made but the results were deemed unreliable, although the experimental approaches developed will prove useful in a future program.

Successful incorporation of amorphous metals into MEMS, such that the unique properties of amorphous metals are fully utilized, will enable the fabrication of MEMS devices with significantly enhanced performance and reliability. Some potential applications envisaged include:

Protective coatings on biosensors

High flexibility, corrosion resistant membranes for pressure sensors

Large throw actuators

Nozzles for high pressure corrosion resistant fluids to withstand pitting and cavitation

Sensors exposed to space and deep sea environments

This seed program has demonstrated that amorphous metals can be successfully incorporated into the standard MEMS process flow such that MEMS devices containing amorphous metals will be fabricable. Only one amorphous alloy has been investigated and other amorphous alloys may prove more suitable for specific applications. Issues such as residual stress control, material property optimization and property characterization remain in need of further work.

2.0 Background and Program Outline

Amorphous metals have received considerable attention since the discovery of compositions that crystallized sufficiently slowly on cooling from the melt that bulk metallic glasses, with no crystalline structure, (BMGs) could be produced. BMGs have now been developed based on Zr, Al and Fe. Typically compositions include several elements with widely differing atomic sizes such that crystallization from the melt is inhibited. The resulting glassy metals have unique properties, such as high strength and strain to failure, a high hardness, and a low coefficient of friction. However, fully amorphous glassy alloys can exhibit low toughness and failure can result from the development and propagation of shear bands that transverse the material leading to premature failure. One issue faced by the desire to use amorphous metals as thin films is whether the shear banding phenomena is more or less critical in the material prepared as a thin film.

The tendency of amorphous metals to develop shear bands can be reduced by heat treatment. Partial or full devitrification into a nanophase microstructure can enhance mechanical properties by precluding the development of slip bands.

At INEEL, iron-based amorphous metals have been developed that can be deposited as coatings by spray deposition processes. These coatings impart high surface hardness, excellent corrosion protection, and low friction and wear properties.[‡] These iron-based amorphous metals are already in use as coatings for steel and coating processes are developed and mature. For this contract, INEEL agreed to provide their materials for evaluation as MEMS materials. We originally envisaged having INEEL coat substrates with DAR 27 using their high velocity oxy-fuel (HVOF) spray deposition system.

Two INEEL compositions, DAR 27 and DAR 27 CB were used in this study. These compositions are proprietary to INEEL and are not included in this report. The DAR27

[‡] INEEL has transitioned this technology to the Nanosteel Co. for further development and commercialization - http://www.nanosteelco.com/

alloy composition was used in initial plasma spray coatings and was used to HVOF coat the targets used in later RSC laser ablation and sputtering studies. DAR27CB was used for the INEEL laser ablated samples. INEEL has developed a heat treatment for these alloys that results in devitrification onto a three-phase nanoscale microstructure that prevents premature failure by shear band propagation and failure.

Our program plan called for INEEL to supply coated substrates to RSC for cohesion and material property characterization. Then RSC provided patterned test structures to INEEL that were coated and returned to RSC for final processing and test. HVOF deposition would have resulted in coatings too thick for MEMS application and RSC had intended to develop appropriate chemical thinning approaches. Once it was clear that HVOF and lower energy plasma spray deposition processes were too energetic and resulted in excess substrate damage to be viable, the coating approaches were changed to laser ablation (pulsed laser deposition) at INEEL and RSC and sputtering at RSC. Of these two approaches, laser ablation is considered to be better able to transfer complex stoichiometry from target to substrate whereas sputtering would be a much lower cost technology to put into practice. These methods resulted in coatings that were sub-micron in thickness and consequently the proposed chemical thinning task was not pursued.

With the technology developed to coat substrates, RSC fabricated MEMS test structures such as cantilever beams and Guckel rings that demonstrated the MEMS process flow that would enable system fabrication with amorphous metal components. These test structures were evaluated and the overall contract results assessed to determine the judiciousness of investing in a larger contract to develop alloys and processes to fabricate prototype MEMS devices for Government evaluation.

3.0 Proposal Statement of Work

Our work plan initially followed our proposed Statement of Work, but deviated once fabrication issues arose. Several proposed tasks proved problematic and contract funds were depleted before all technical challenges had been resolved. However, with supplemental contract provided by DARPA, most contract goals were achieved, with some dramatic successes. In particular, the quality of amorphous metal structures fabricated using classic photolithography, masking, and etching techniques was very high, with excellent edge definition of the metal.

3.1 Preparation of Detailed Work Plan (All)

The team will review candidate existing iron-based compositions and thermal deposition parameters and finalize the composition, deposition parameters and heat treatments that will be followed at INEEL. This plan will be formalized at the telephone conference call kick-off meeting that will include the Government customer.

3.2 Preparation of Substrates (RSC)

RSC will prepare and provide substrates to INEEL for amorphous metal deposition. The selection of substrate materials, adhesion layers, and surface patterning characteristics will be designed to optimize adhesion of the amorphous metals. Pattern test structures will be incorporated onto the substrates and will include sacrificial layers for evaluation of MEMS device characteristics.

3.3 Coating Deposition (INEEL)

Ingots of the chosen composition will be made and then processed into powder. The powder will then be sieved and air classified to produce appropriate feedstock for thermal deposition. Coatings will be deposited primarily through high velocity oxy-fuel (HVOF) onto the substrates provided by RSC. Spray parameters will be optimized to produce coatings containing a high percentage of glass with minimal porosity. Additionally, studies will be done to evaluate adhesion to the RSC supplied silicon based substrates, that may be enhanced by first spraying onto roughened or selectively roughened substrates or by starting with silicon substrates precoated with metals. Once spray parameters and conditions have been optimized, the coatings will be supplied to RSC in both the as-sprayed amorphous and heat treated (either partially or fully devitrified) conditions. Physical metallurgical studies of the coatings will be done using techniques such as thermal analysis, X-ray diffraction / Rietveld refinement, and microscopy (optical and SEM).

3.4 Chemical Processing (RSC)

Here, the electrochemical thinning and machining requirements will be addressed by establishing, the electrochemical process characteristics. This will include DC polarization for each of the amorphous and devitrified samples in 4 M $NaNO_3$ and 4 M $NaClO_4$ and pulse polarization for amorphous and devitrified specimens in the above electrolytes at two duty cycles. The current efficiency and dissolution morphology will be evaluated by, for example, profilometry or gravimetric methods.

This machining approach is presumed to be amenable to both the bulk film thinning and the anodic masking that will enable the accurate machining of complex shapes. The anodic masking/electrochemical machining procedure will be included within the scope of this proposed effort, although the fabrication of actual devices will not be included here.

Finally, a corrosion evaluation will be conducted using electrochemical impedance analysis in a test solution with exposure times of one week.

3.5 Property Screening (RSC)

Device structures will be released from the substrates as required and material properties such as adhesion, stress, resistivity, etc., will be assessed for suitability for use in MEMS devices. The substrates will be removed by appropriate etching techniques to enable tensile testing. Tensile tests will be performed to obtain the stress-strain relations, the elastic modulus, and Poisson's ratio. Hardness, yield strength, and other materials properties of interest will be measured. Microscopy (light and scanning electron microscopy) will be used to examine fracture surface morphology and establish failure mechanisms. The detailed measurement of wear rates and friction coefficients, and the determination of wear mechanisms and failure modes of the materials under various conditions of speed, contact stress, temperature, and environment is anticipated to be beyond the scope of this preliminary effort, although a preliminary assessment of these properties will be included.

3.6 Device Fabrication Issues (RSC)

In this task, the suitability of amorphous metals for MEMS applications will be assessed. This will include an analysis of the material requirements for device structures and an assessment of the fabricability of the INEEL materials into MEMS devices. A process sequence for the microfabrication of amorphous metals into MEMS devices will be developed.

3.7 Reporting (All)

Consolidated technical progress reports as required and a Final Report will be prepared for the Government. The Final Report will incorporate an assessment of the suitability of amorphous metals for MEMS devices and an assessment of the

value to DARPA of awarding a follow-on program that would address this topic in significantly greater detail and that would include process scale-up and device fabrication and test tasks.

3.8 Program Management (RSC)

The separate program tasks will be coordinated and resources allocated to each task as necessary to ensure program success. Regular telephone conference calls and e-mail distributions with the participants and customer will ensure effective technical data exchange.

4.0 Substrates and Substrate Coating Optimization

4.1 Selection of Substrates

Silicon-based substrates were prepared for the deposition of the amorphous metals. Silicon substrates with and without coatings of silicon dioxide, silicon nitride, nickel, and aluminum, as well as uncoated sapphire and silicon on insulator substrates were supplied by RSC to INEEL. The coated substrates were returned to RSC for testing of wafer level stress, adhesion, abrasion, sheet resistance, corrosion, and tribological properties. The sample type and its intended purpose are shown in Table 1. Coating thicknesses were typically ~5000 Å (0.5 μm).

Table 1. Type and Purpose of Substrates For Amorphous Metals Materials Property Studies

Sample	*Quantity*	*Purpose*
Uncoated Si	30	Tensile test structures, magnetic measurements, adhesion, stress, tribology
Si with Ni coating and Al sacrificial structure	4	Electrochemical processing studies
Si with Ni coating and SiO_2 sacrificial structure	4	Electrochemical processing studies
Si with thermally deposited SiO_2	8	Corrosion, sheet resistance measurements
Si with PECVD SiO_2 coating	4	Adhesion
Si with PECVD Si nitride coating	4	Adhesion
Si with Ni coating	4	Adhesion
Si with Al coating	4	Adhesion
Sapphire	8	Adhesion
Silicon on insulator	4	MEMS processing studies

4.2 Plasma Spray and HVOF coating of Substrates

The first spraying was done on uncoated silicon substrates. Spraying was done with a DC plasma torch since the velocities are much lower than HVOF spraying and the lower velocity were anticipated to cause less surface damage. Additionally, plasma spraying

enables better control of residual stresses in the coating and a wider range of particle sizes can be fed through the gun system and deposited. This spraying was done with a DC plasma torch using atomized particles of alloy DAR27 which were air-classified to yield particles from 23 to 53 microns. Due to the high velocity of the plasma process, excessive surface damage including roughening and cracking occurred in the silicon substrate. The steel coating also spalled off upon cooling. Based on these results a series of spray studies were initiated using fine (<22 μm) particles of alloy DAR27 in order to minimize substrate damage from kinetic impact.

After spraying, there was evidence that the surface of the silicon was indeed less damaged by using the smaller particles. However, the steel coating did not bond sufficiently with the silicon. In some cases, areas of the coating stuck to the silicon surface but this coating is not adhered on sufficiently for further studies. Two main problems were identified with coating amorphous steel onto silicon. The first is the nature of the bonding which is primarily metallic in the steel and primarily covalent in the silicon which makes it difficult to form effective bonds. This effect is compounded in the DAR27 alloy, due to its high atomic fraction of P-Group (C, Si, and B) elements. These elements will act to fill up the free electron energy band in the metal dramatically reducing the already limited ability of the metal to form covalent bonds. The second factor is the large difference in thermal expansion between silicon and the steel which can cause coating delamination upon cooling.

The next set of spray studies was done on the nickel-coated (0.5 μm) silicon samples. The plasma spray system with the fine particles were used with spray parameters which were most promising from the previous studies. While the initial spraying seemed promising, the coating again spalled off upon cooling. Examination after spraying showed that the silicon substrate was bare and the nickel was adhered to the steel coating. Thus, it appears that the nickel / steel bond was much stronger than the silicon / nickel bond.

RSC additionally supplied masks for directly depositing “dog-bone” shaped samples for tensile property studies. These masks were used to spray the amorphous steel onto aluminum and eight such tensile specimens were made. The aluminum substrate was selected since it can be readily removed by etching in a NaOH solution.

4.3 Coating of Substrates by Laser Ablation at INEEL

All attempts to optimize the plasma spray deposition conditions still resulted in poor adhesion and damaged substrates. Therefore, the next set of spray studies was done using laser ablation. The laser ablation system was expected to impart less damage on deposition, the coating on silicon would be very thin layer and previous studies at INEEL have indicated that the chemical stoichiometry can be maintained during the ablation process so that amorphous coatings would still be obtainable.

Several iterations of coating silicon with DAR27 steel using the INEEL Pulsed Laser Deposition (PLD) system (Figure 1) were made. Substrates, to be used as targets, were prepared by depositing a DAR27 coating onto a 4340 base steel coupon using HVOF. The targets were then hit with a 200 mJ laser at 20 Hz. Depending on the focus of the beam and the laser operating parameters, thick coatings have been deposited up to 3 μm in thickness. Typically, it took from 1 to 2 hours to build up a 1 μm steel coating on a silicon substrate. When optimized, this produced a very well adhered coating which could not be scraped off using simple tools. It was found that the temperature of the coating deposition was crucial for developing high bond strengths. Too high a temperature, and the steel degrades the silicon and too low a temperature and the coating does not bond effectively. From visual inspection, the coatings as-deposited were uniform, but it was found that the surface roughness and topography varied significantly depending on operating conditions.

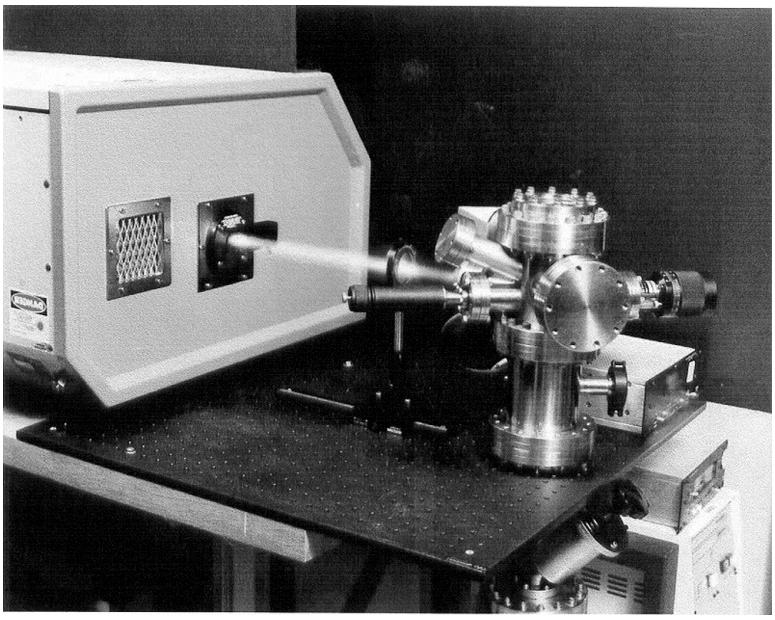

Figure 1 The Pulsed Laser Deposition (PLD) System used at the INEEL to deposit steel coatings onto the silicon substrates. Note that the focused beam of the laser can be seen before it enters the PLD system.

At this stage in the contract, many issues remained in obtaining the defect free uniform coatings necessary for MEMS. However, there was enough evidence to show proof of principle that amorphous steel technology can be successfully married to silicon for potential MEMS devices.

The following data all pertains to one particular silicon sample coated with DAR27 steel using the INEEL PLD System. A silicon target was coated with a ~1 µm thickness of steel by ablating a HVOF coated DAR27 substrate with a focused 200 mJ laser at 20 Hz. The scanned image of the surface of the coating can be seen in Figure 2. An X-ray diffraction scan was done on the as-deposited surface from 20 to 85° with a 0.01° stepwidth and 5 seconds counting time per step. The diffraction scan showed a broad hump indicating that an amorphous structure was formed (Figure 3). Note that the only Bragg diffracted peak was the (400) from the silicon substrate.

The coated silicon coupon was then heat treated in a vacuum at 700°C for 1 hour. After heat treatment, an X-ray diffraction scan was taken using the same conditions as before (Figure 4). In the diffraction scan, the multitude of sharp crystalline peaks indicate that

several phases, probably nanoscale, formed after crystallization. The heat treated pattern was analyzed using Rietveld analysis until a good fit was obtained with a total Chi-squared of 1.4 (Fig. 5). The devitrified DAR27 was found to consist of 4 phases; □-Fe, $Fe_{23}C_6$, Fe_3B, and Fe_2B (Table 2). The results are similar to what has been found from previous studies on DAR27 HVOF coatings. The only difference was the addition of a new phase Fe_2B. Note that this phase has been found in other alloys of this type and is the stable phase in the Fe-B binary system. The surface of the heat treated coupon was observed in the SEM to determine the uniformity of the coating (Figure 6). While the bulk of the structure is uniform on a 200 nm length scale, some larger particles can be seen at the surface. An EDS scan was taken at the surface of the heat treated coupon (Figure 7). In the coating Fe, Cr, W, and Si were positively identified with Mo and Mn probable. The identified and probable elements match the starting components of the DAR27 alloy. Since the coating formed a glass upon deposition and devitrified to a similar structure to that found before, it is probable that the composition changed little from the targeted value of the starting alloy.

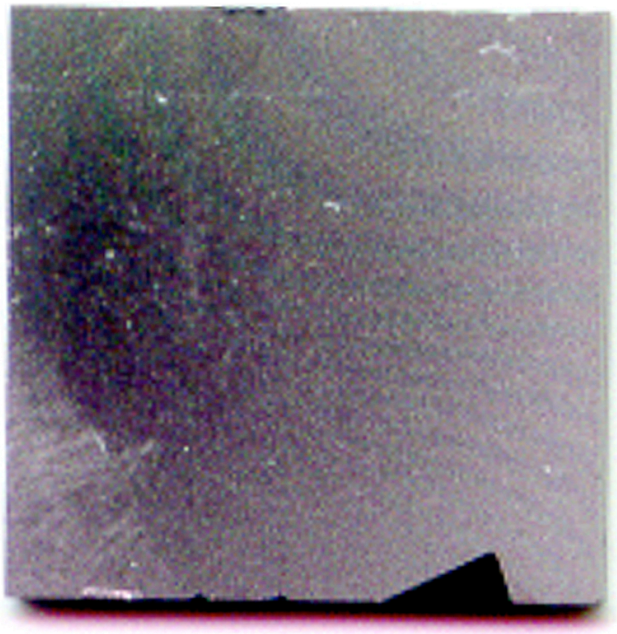

Figure 2 A scanned image of the surface of the PLD coupon coated with □ 1 μm DAR27 steel. Note at the bottom right, the clip mark where the silicon substrate was held down during coating can be seen.

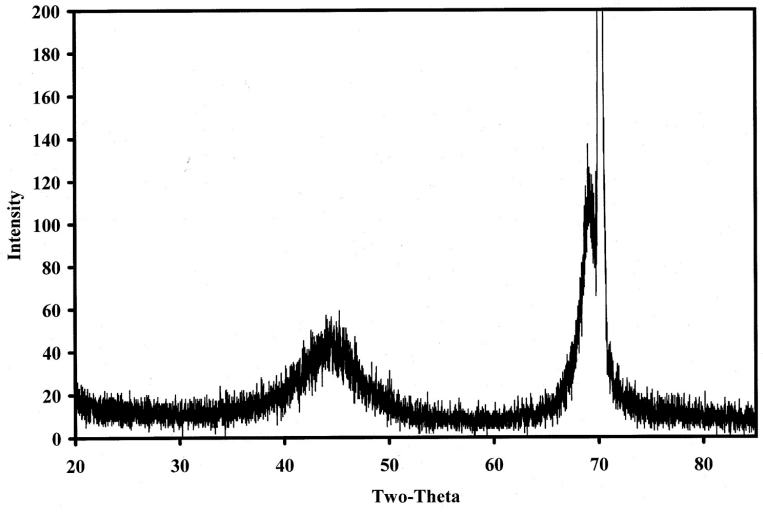

Figure 3 X-ray diffraction scan of the as-deposited steel coated silicon coupon. The broad hump centered near 45° indicates that an amorphous structure was formed. Also, note that the silicon (400) reflection from the substrate is shown off scale.

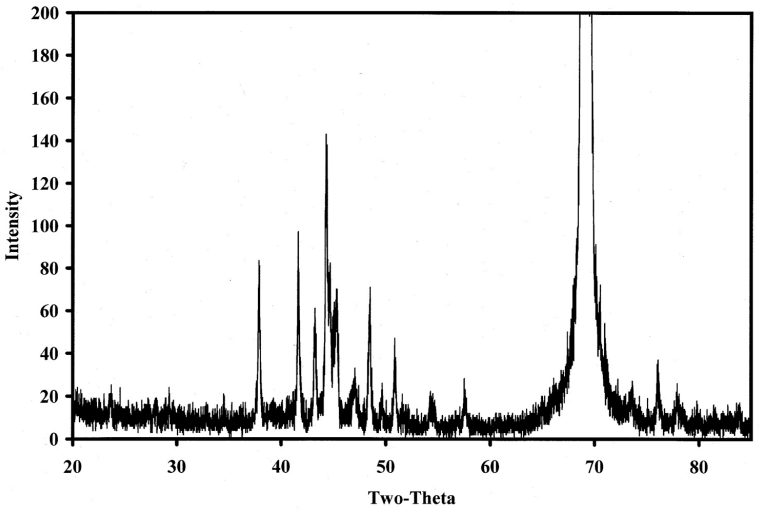

Figure 4 X-ray diffraction scan of the steel coated silicon coupon which has been heat treated at 700°C for 1 hour. The many sharp crystalline peaks indicates that several nanoscale phases formed after crystallization. Also, note that the silicon (400) reflection from the substrate is shown off scale.

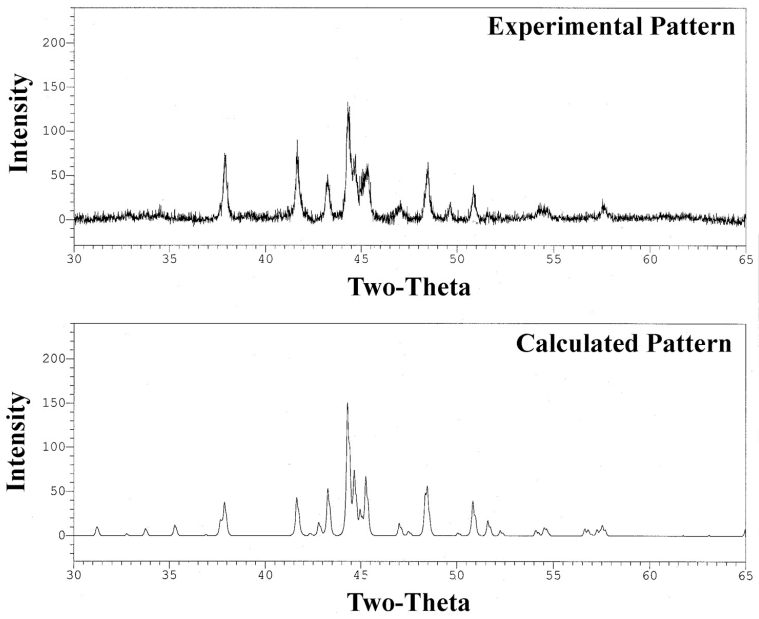

Figure 5 Experimental and calculated pattern for the heat treated PLD coated silicon coupon. Note that the total chi-squared error over this angular range is 1.4.

Table 2 Phases Found in PLD Coating Heat Treated at 700°C for 1 hr

Phase	Crystal Structure	Space Group	Lattice Parameter(s) (Å)
□-Fe	cubic	Im3m	a = 2.867
$Fe_{23}C_6$	cubic	Fm3m	a = 10.614
Fe_3B	tetragonal	I-4	a = 8.636, c = 4.267
Fe_2B	tetragonal	I4/mcm	a = 5.083, c = 4.222

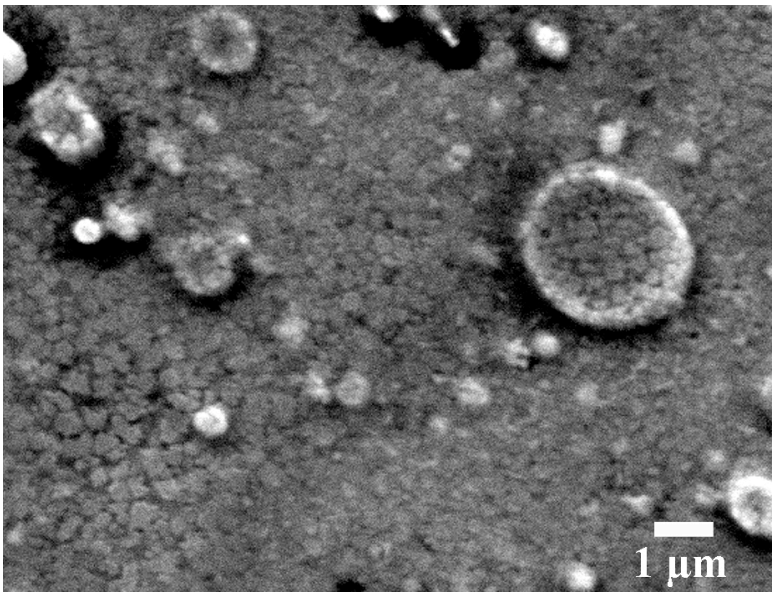

Figure 6 SEM micrograph showing the detail of the heat treated PLD steel coated silicon. While the bulk of the structure is uniform on a 200 nm length scale, some larger particles can be seen at the surface.

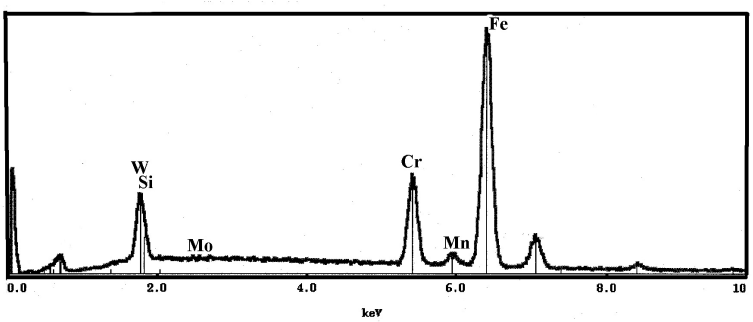

Figure 7 EDS scan from the surface of the heat treated PLD steel coated silicon. The following elements were positively identified in the coating, Fe, Cr, W, and Si with more work needed to clarify the Mo and Mn content.

4.4 Amorphous Metal Deposition at RSC

INEEL delivered as-deposited silicon coupons, heat-treated coated coupons and coated, prepared test structures to RSC for further evaluation. These structures all contained spatter defects typical of laser ablation (or pulsed laser deposition) as depicted in Fig. 8

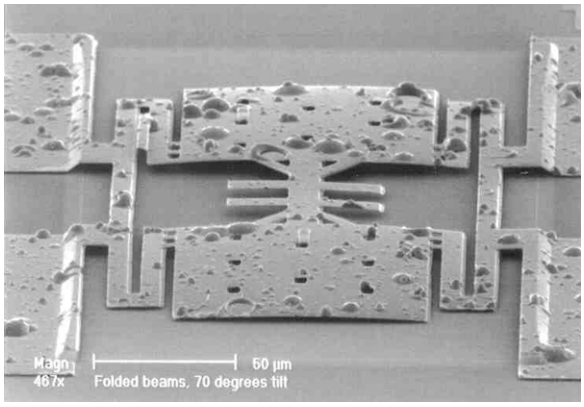

Figure 8 – Test structure after post-laser-ablation processing at RSC, showing spatter defects typical of laser ablation processing.

Clearly, the quality of the coated amorphous metals with the spatter defects was not adequate for the MEMS application and further work was performed at RSC, addressing both laser ablation and sputtering to improve on the coating quality. For this work, INEEL prepared both laser ablation targets and sputtering targets.

4.4.1 HVOF coating of Laser Ablation and Sputter Targets

For this effort, INEEL used the HVOF coating method to deposit 3 mm thick coatings of the DAR 27 composition onto both a disk-shaped aluminum sputtering target and steel rod laser ablation target. DAR 27 was selected as that is the optimized composition for HVOF coatings.

4.4.2 Coating of Substrates by Laser Ablation at RSC

RSC used its laser ablation facility to coat silicon using the DAR27-coated steel target prepared at INEEL. For the deposition, a 248 nm wavelength laser with a 30 nsec pulse width, 7 Hz repetition rate, focused onto the target with an approximate energy density of 1.5 J/cm^2. The target-substrate distance was 12.5 cm, and the substrate temperature 20°C

Using this technique, the coated silicon substrates had none of the spatter defects associated with the earlier laser ablation studies, as depicted in Fig. 9.

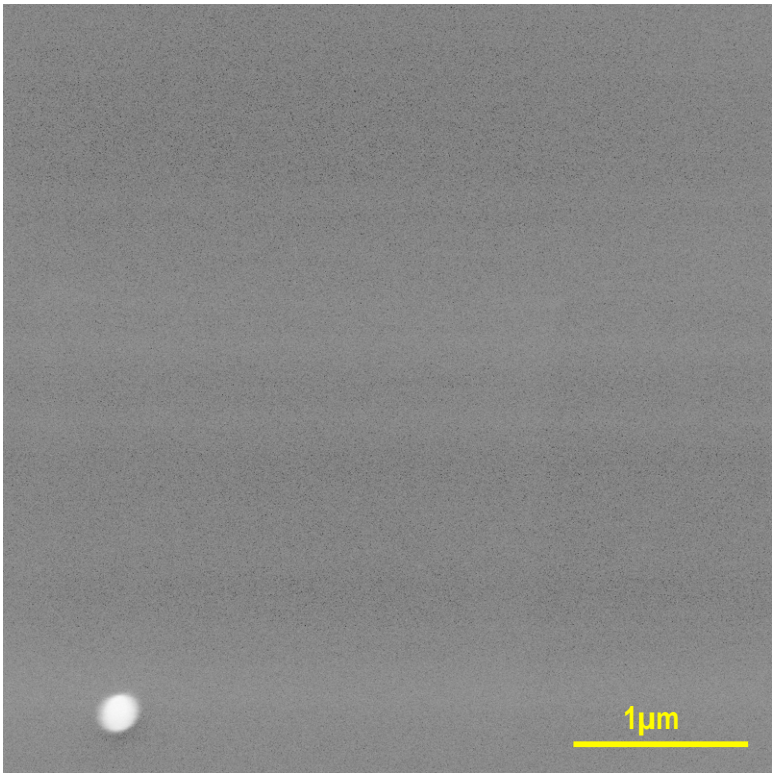

Figure 9. DAR 27 coated silicon coated by laser ablation at RSC. No spatter defects observed at 20,000 x. The image region was selected to include small charging artifact.

4.4.3 Coating of Substrates by Sputtering

Sputtering DAR27 onto Si was also investigated at RSC as a lower cost and more scalable alternative to laser ablation. INEEL used HVOF to deposit 1/16" DAR27 onto a 3 in diameter sputter target that was then used at RSC to deposit 0.6 µm thick coatings onto silicon substrates using RF magnetron sputtering in pure argon. By using 3-inch diameter targets, the RSC sputtering facility enables coatings with thickness variations of <7% to be deposited onto 3" wafers. In addition, coatings can be deposited onto substrates that are either water cooled or heated up to 700°C. Inspection by SEM revealed no defects as can be ascertained from Fig. 10.

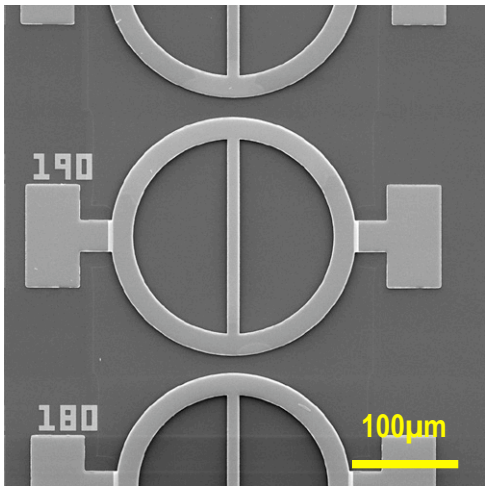

Figure 10. Guckel rings deposited by sputtering.

5.0 Material Processing and Structure Fabrication

5.1 Electrochemical processing

The originally envisaged electrochemical tasks were to develop processes for thinning the as deposited DAR27 coatings and to develop a process for electrochemically "writing" a structure onto the coated substrate. The thinning requirement was predicated on coating substrates with DAR27 tens of microns thick since HVOF plasma spraying was envisaged as the primary coating approach. Once laser ablation and sputtering were identified as viable coating methods, the chemical thinning requirement was no longer a requirement although the ultimate need to "write" structures onto a coated substrate remained an identified need.

Pulsed electrolysis in environmentally benign 4M $NaNO_3$ was first approach used. During positive part of cycle, Fe passivates (oxidizes to Fe_3O_4) and water is electrolyzed to form a reactive layer of proton ions (H^+) at the surface. During negative part of cycle the Fe_3O_4 dissolves, and Fe goes into solution under chemical polishing conditions as $Fe^{2+.}$ Preliminary results indeed indicated that this approach is viable to "write" nanostructures on a DAR 27 coating using a probe electrode to define regions for dissolution

A second task evolved to support the preparation of tensile samples for which an approach was needed to lift-off of the amorphous metal coatings from silicon substrates. Technology was developed to back etch silicon to lift-off the DAR27. Initial tests were conducted with Ni-coated Si for which lift-off was readily achieved by exposing the coated silicon to 44g/100ml KOH @ 85°C. However, DAR27 remained attached when exposed to KOH solution under identical conditions and required complete dissolution of the silicon for lift-off. Clearly, DAR27 forms a very chemically resistant bond to silicon that bodes well for environmental reliability

5.2 Test Structure Fabrication and Process Flow

Patterned polyimide MEMS structures were fabricated on silicon substrates to fabricate test MEMS structures incorporating amorphous metal films. The structures were patterned using dry etch techniques. Thin films of amorphous metal were deposited onto the patterned structures. The polyimide structures were subsequently removed using a wet chemical etch to produce free standing Guckel rings, clamped-clamped and single-clamped cantilevers of amorphous metal. These structures were fabricated with a 0.5 μm layer of SiO_2 at the interface between the Si substrate and the amorphous metal. The structures for residual stress measurement do not require the insulator layer but resistivity structures, which do require an insulator layer, were fabricated on the same wafers for maximum process efficiency. The insulator layer would not be expected to affect the stress measurements.

A schematic of the process flow is depicted in Fig. 11

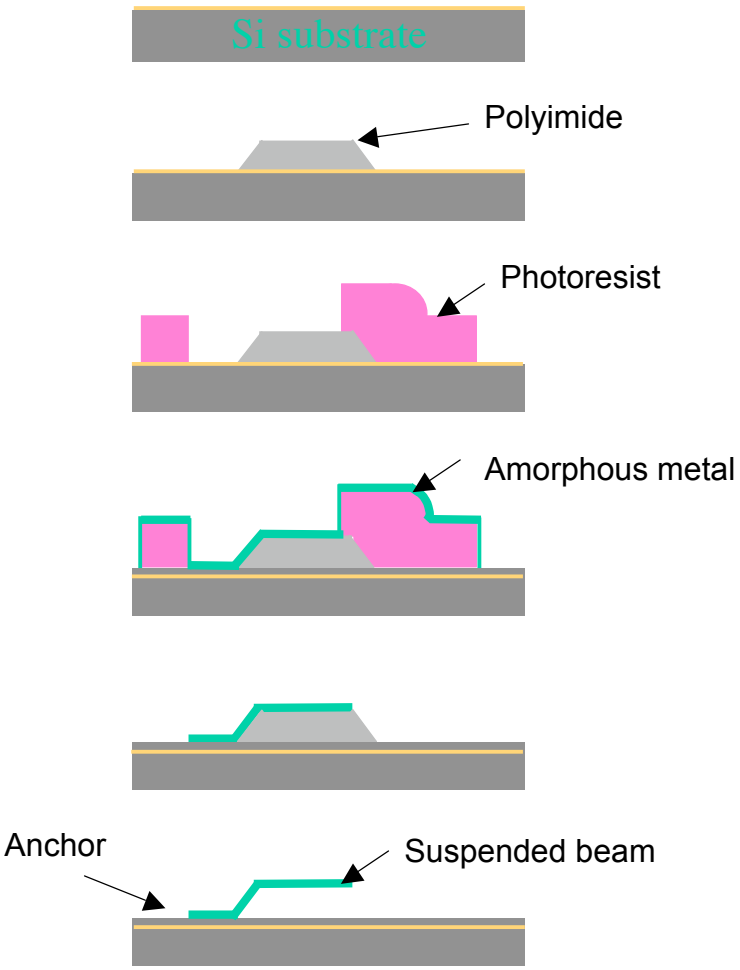

Figure 11 MEMS structure fabrication process flow

A silicon wafer coated with ~0.5µm SiO_2 was used as the starting substrate material. A ~3.7 µm thick polyimide (PI) sacrificial layer was spun-coat, baked and patterned. A second ~4 µm thick layer of photoresist was spun-coat and patterned. This became the substrate for the laser ablation and sputtering depositions of DAR27.

Unwanted metal film was removed by lift-off (acetone dissolution of the photoresist). The excess amorphous metal lifted cleanly away. The sacrificial PI was then removed by an oxygen plasma etch, leaving the suspended structures.

Dimensions of the MEMS test structures fabricated follow:

Single-clamped beams (cantilevers):

widths: 10 or 20 □m

lengths: 45-125 □m, in 10 □m steps and 125-345 □m in 20 □m steps

Double-clamped beams (used for films held in tension):

widths: 10 or 20 □m

lengths: 40-120 □m, in 5 □m steps and 120-250 □m in 10 □m steps

Double-clamped rings (used for films held in compression):

width: 10 □m

lengths: 50-120 □m in 5 □m steps and 120-250 □m in 10 □m steps.

Images of test structures are reproduced in Fig. 12. These images were of laser ablated depositions fabricated at INEEL and show evidence of the spatter defects that were eliminated after further process development.

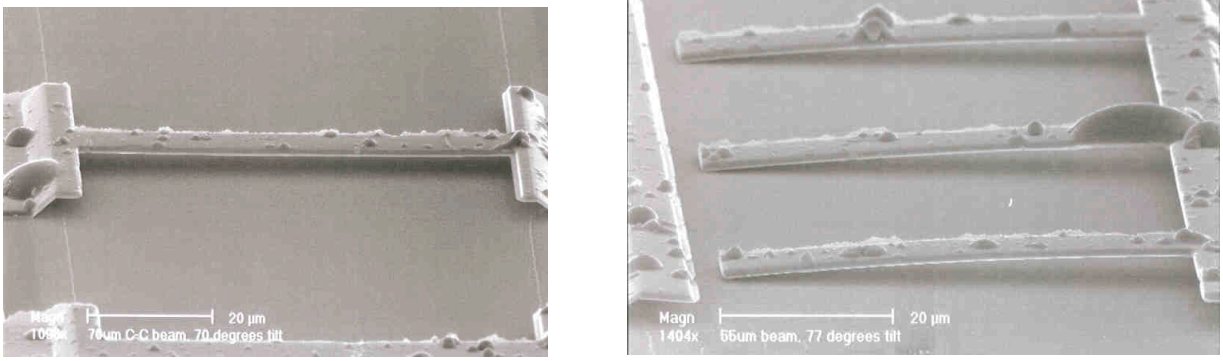

70 µm double cantilever beam 65 µm cantilever beam

Figure 12. A double cantilever beam that has bowed slightly, indicative of an overall residual compressive stress and a single ended cantilever beam that has curved downwards, indicative of a stress gradient across the thickness of the beam.

Such structures were first demonstrated using patterned substrates coated by laser ablation at INEEL. Later, similar structures were made by coating patterned substrates by both laser ablation and sputtering at RSC. Examples of structures coated at RSC are depicted in Figs. 13. The spatter defects typical of laser ablation were eliminated with use of RSC developed procedures for laser ablation.

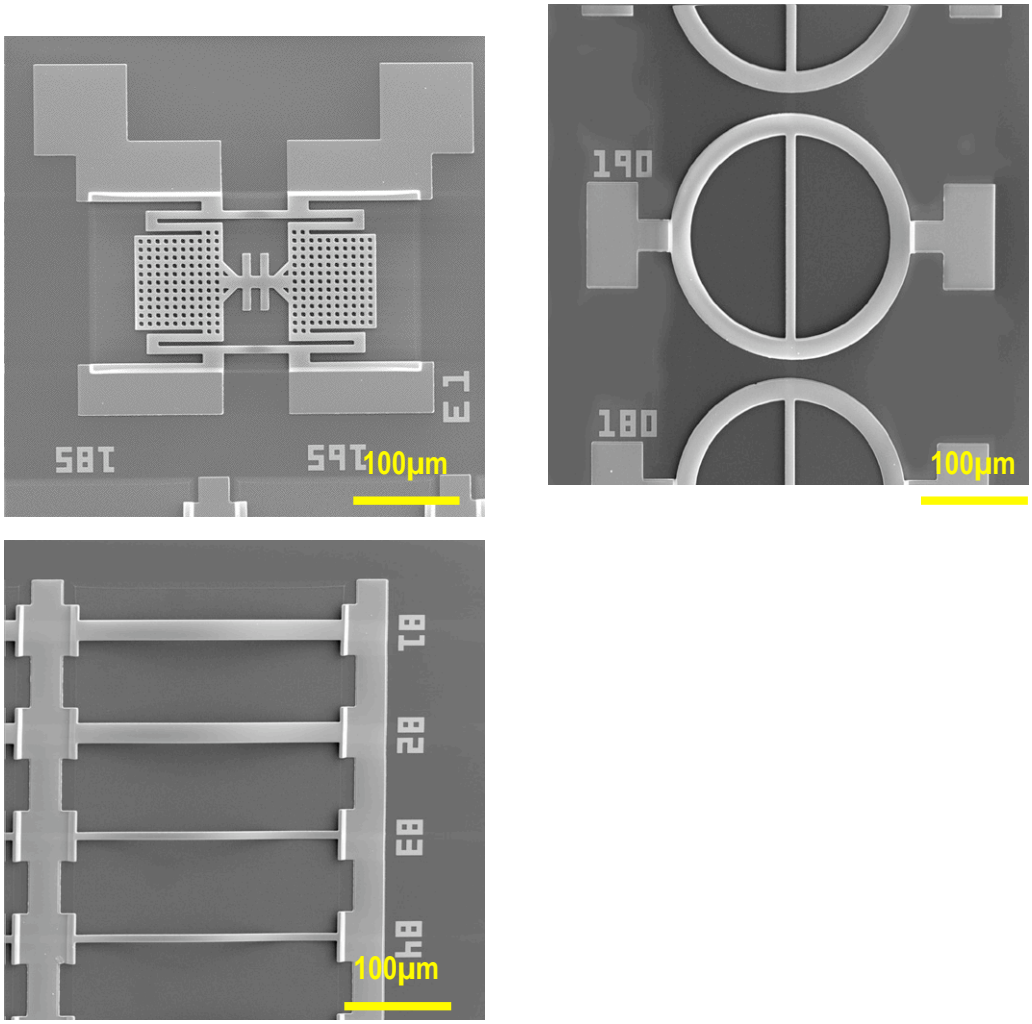

Figure 13. Structures fabricated at RSC using laser ablation. Samples were unannealed after fabrication.

We have clearly demonstrated that the laser ablation of amorphous metal deposition is compatible with MEMS fabrication techniques, such as photoresist patterning and polyimide etching-based processing. With this approach, DAR27 attachment points remained well adhered to the silicon substrate after processing. Key to this success is that RSC has developed laser ablation so that spatter defects can be eliminated.

Using these methods, suspended structures, such as beams, rings and more complex structures can be made using standard MEMS fabrication techniques. However, at this stage of process development, the DAR27 coatings exhibit a through thickness stress gradient superimposed on an average tensile residual stress. These stresses may be controlled by changing deposition conditions and this will need to be addressed in a future program.

Sputtering was also evaluated for the deposition of MEMS structures. Several broken cantilevers present in the MEMS test structures demonstrated the existence of a stress gradient in the as-deposited films. Again, this stress gradient is tailorable and can be largely eliminated by change of process conditions. This, too, will need to be addressed in a future program.

The sputtered structures also exhibited some incomplete photomask removal whereas the laser ablation method produced clean samples. Residual stress in all these deposited films remains an outstanding issue.

6.0 Material Property Measurements

Amorphous or amorphous derived metals have properties that can be very different from their crystalline counterparts. Since mechanisms for crystalline slip are absent, fully amorphous metals typically exhibit little plasticity before failure. Failure is, however, preceded by the formation of slip bands. Slip band formation can be impeded by heat treating amorphous metals to partially or fully devitrify them to either a ductile phase reinforced glass or a nanocrystalline multiphase alloy.

INEEL has developed a heat treatment that fully devitrifies DAR27 into a three phase, nanocrystalline solid that has optimum properties as a bulk solid. Here, we examined both as-deposited amorphous DAR27 and the heat treated, nanocrystalline DAR27 described in Section 4.3.

6.1 Hardness by Nanoindentation

Silica coated silicon substrates were coated with ~0.4μm thick DAR27 by laser ablation at INEEL. These were evaluated using nanoindentation in the as-deposited and annealed (600°C for 10 minutes) state. Figure 14 contains three sets of curves, a set for the substrate only (SiO_2 coated silicon), a set for as-deposited DAR27 and a set for the heat-treated DAR27.

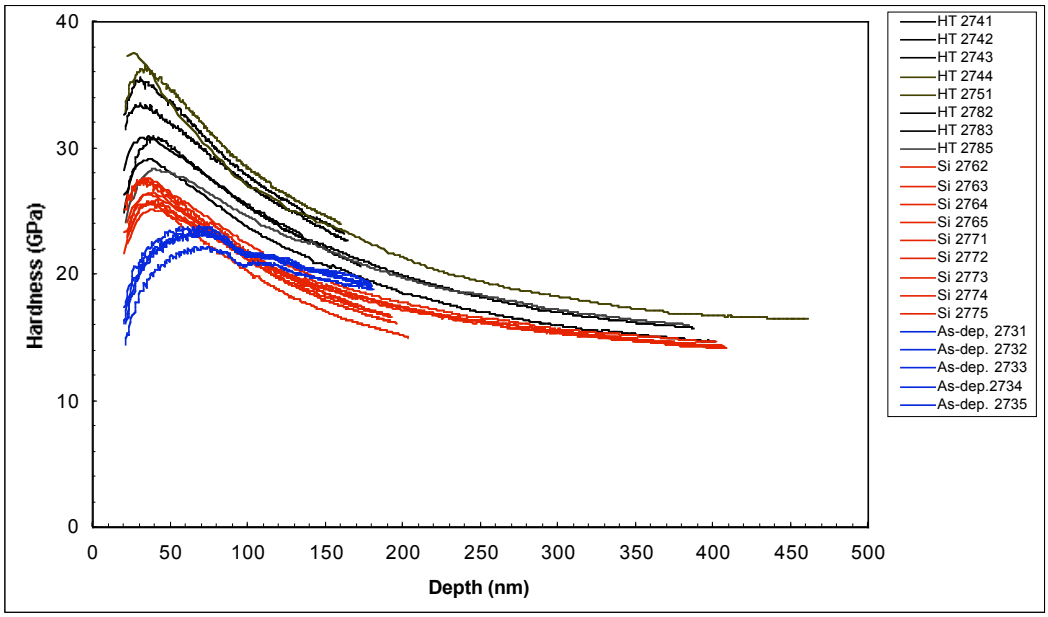

Figure 14 Nanoindation curves for DAR 27, unannealed and annealed for 600°C for 10 minutes. Uncoated substrate material was used for comparison.

The nanoindentation hardness curves for the substrate only displayed behavior typical for silicon, and of the three sets of data, the heat-treated amorphous metal had the highest peak hardness values. The as-deposited amorphous metal had a lower peak hardness with a reproducible but unusual decay characteristic after the hardness peak that was attributed to shear band development. The DAR27 coating thickness was approximately 400 nm and experience with other nano-indentation experiments on thin coatings suggests that the silicon substrate would influence the nano-indenter response after ~150 nm penetration.

Vickers indentation was used to evaluate the adherence of the DAR27 to the substrate by initiating spalling. Figure 10 shows two Vickers indents made on the surface of the as-fabricated and heat treated coatings. The indents reveal cracks developing in the coating that may or may not penetrate the silicon substrate. A small piece of coating had spalled from one corner of the heat treated indent.

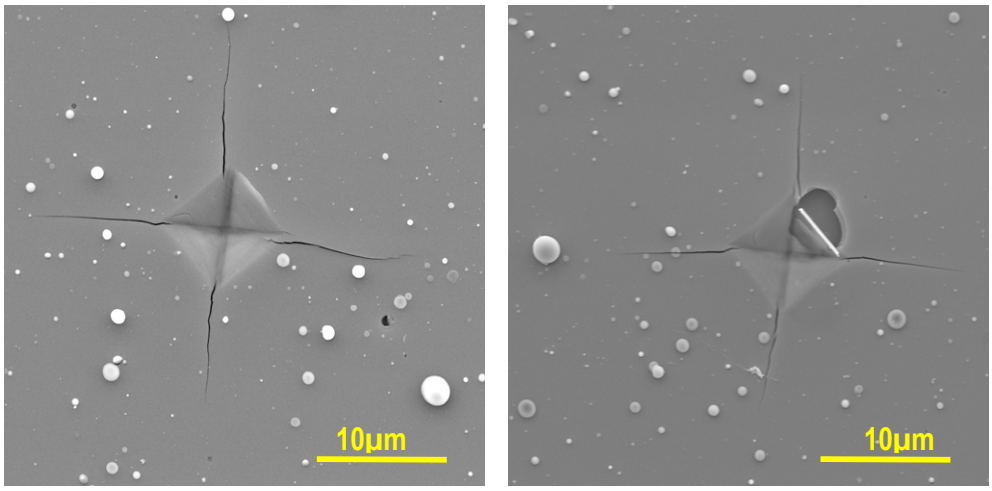

Figure 15. Vickers indentation of DAR27 deposited by laser ablation at INEEL. The left image shows an indent in as deposited film and the right image shows an indent with a small spalled region in a sample heat treated for 10 minutes at 600°C in air. The indentation load was 50g.

6.2 Magnetic Measurements on Amorphous Metals

An F.W. Bell hand-held Gauss/Tesla meter (model 4048) was used to measure the dc magnetic field of as-deposited and devitrified samples (10 min anneal at 600C) of DAR27 deposited onto silicon substrates. The probe was zeroed in a zero-gauss chamber, then a 4 kGauss magnet was used as the probe reference. Readings on all the samples were ~1 gauss, essentially the same as the background reading with no sample.

An attempt was made to magnetize one of the as-deposited samples by placing it on the 4 kGauss magnet. When the sample was removed and tested, the reading was still ~1 gauss. It was not possible to induce a magnetic field.

6.3 Corrosion Studies

The corrosion resistance of the DAR27 (as-fabricated and heat treated) was compared to that of Type 304 stainless steel and 1010 carbon steel. The environments used were Harrison's solution (a simulant for acid rain) and $NaHCO_3$ buffered 0.6M NaCl that had previously been used to characterize certain stainless steels). The corrosion resistances were measured and the DAR27 was found to be comparable to stainless steel in

Harrison's solution (as would be expected given that compositions were similar) and DAR27 showed superior pitting resistance to stainless steel in the NaCl tests. The pitting potential for DAR27 was 400mV above that of 304 stainless steel - a significant increase. The corrosion resistance for the materials compared is included in Table 3 and Fig. 16.

Table 3 Corrosion resistance of DAR27CB compared with mild steel and stainless steel.

Alloy	R_{corr} □ cm^2
1010 Steel	250
DAR27CB	13000
304 S Steel	16000

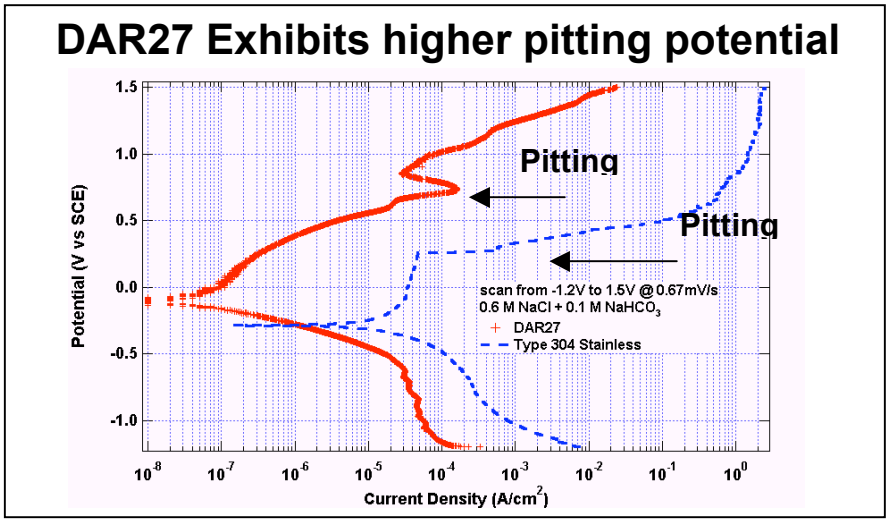

Figure 16. Plots of pitting potential for DAR27 and Type 304 stainless steel.

6.4 Tribology Experiments

The RSC tribometer consists of a calibrated rotating wheel that impinges on a flat sample. Wheel has curved circumference such that the wear patch is circular dimple. Measured data consist of retardation forces opposing direction of circumferential motion

and the normal forces applied. The scale of our experiment proved too small for our tribometer and we were operating in the noise. Useful data was not obtained.

We envision that we can modify a machine for TEM specimen preparation, known as the Dimpler, to provide similar data at a scale appropriate for MEMS material development. However, this was beyond the scope of the present effort.

6.5 Atomic Force Microscopy Characterization (AFM)

The AFM can be used to apply a controlled, low-force application of a diamond tip mounted on a high stiffness (~200 Nt/m) cantilever over a well-calibrated, large range of force (10^{-6} - 10^{-4} N) Thus, in addition to high resolution imaging offered by the AFM, the technique enables the measurement of microhardness with high spatial resolution, direct measurement of compliant flexure in cantilever beams, microtribology, as well as measurement of micro-contact resistance. Measurements were made of modulus and residual compressive stress using the geometrical relationships shown in Fig. 1.7.

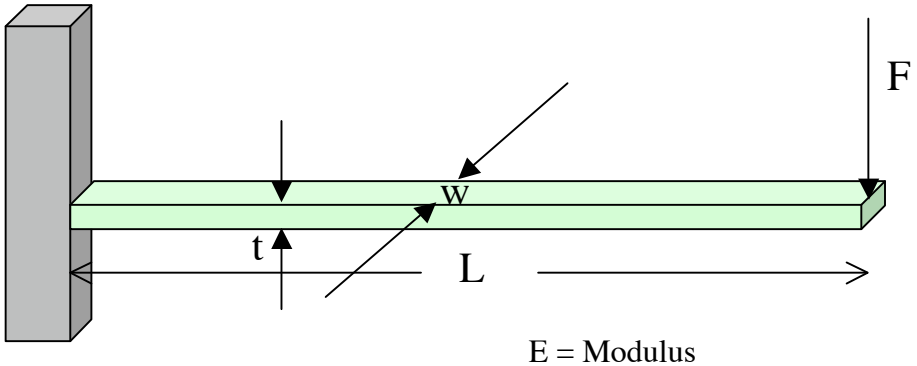

$$E = \left(\frac{F}{\delta}\right)\frac{4L^3}{wt^3}$$

E = Modulus
F = Applied Force
□ = End deflection
L = Length
w = Width
t = Thickness
F/□ = Spring Constant (AFM data)

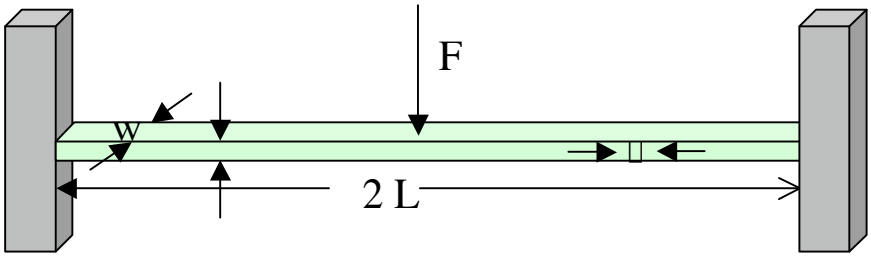

$$\left(\frac{F}{\delta}\right)\frac{L}{\sigma w t}\left[1-\frac{\mathrm{Tan}\left(\frac{L}{t}\sqrt{\frac{3\sigma}{E}}\right)}{\left(\frac{L}{t}\sqrt{\frac{3\sigma}{E}}\right)}\right]=1$$

□ = Residual compressive stress
E = Modulus
F = Applied Force
□ = Mid-point deflection
2L = Length

Figure 17 Determination of modulus from deflection of single and double cantilever beams.

The AFM technique was used here to measure stiffness of the DAR27 cantilever beams that were part of the MEMS test structures made using laser ablation at INEEL. In the unannealed state, the modulus was 1410 GPa but after annealing for 600°C for 10 minutes, the modulus was 470 GPa.

The residual compressive stress in the double cantilever beams is reported in Table 4.

Table 4 Residual compressive stresses in selected double cantilever beams

	2L = 150 μm	**2L = 100 μm**	**2L = 50 μm**
(Unannealed)	**73 MPa**	**256 MPa**	**1142 MPa**
(Annealed)	**35 MPa**	**103 MPa**	**240 MPa**

6.6 Tensile Test Development

Clearly, one of the key properties relevant to the successful incorporation of amorphous metals into MEMS devices are the tensile mechanical properties (strength, elastic limit, strain to failure). Several approaches were pursued and a tensile test procedure was developed but not optimized. The main challenge faced was the fabrication of traditional, albeit undersized dog-bone shaped tensile specimens of the amorphous metal.

In the first approach, coatings of amorphous metal were deposited through a dogbone-shaped window onto aluminum substrates. Aluminum was chosen for ease of subsequent dissolution in a KOH bath. DAR27 coatings were successfully deposited, but residual stresses in the coating caused the released films to scroll up tightly such that efforts to uncurl them led to their failure.

In later efforts, RSC deposited DAR27 directly onto silicon substrates by the laser ablation method. Technology was then developed to back etch the silicon as an approach to DAR27 lift-off. Initial tests with Ni-coated Si resulted in the nickel readily lifting off from the silicon when exposed to the 44g/100ml KOH solution at 85°C. Under identical conditions, DAR27 remained attached and complete dissolution of silicon turned out to be necessary for lift-off. However, once the DAR27 had been released from the

substrates, the films again were observed to scroll up and become impossible to mount in a tensile frame.

To mitigate against the scrolling, “window frames” of copper, attached to the top face of the dog-bone such that the tensile gage section remained free, were evaluated. With such “window frames” the tendency for scrolling on release from the substrate would be prevented. A MEMS mask consisting of PMGI/silicon oxide for deposition of structures was designed and fabricated. Amorphous metal films of thickness ~1 micron were deposited and patterned onto silicon substrates.

Initially, an electrodeposited copper frame with a gap on each side of the frame was deposited onto the dog bone-shaped amorphous metal film, as shown in Fig. 18. The gap was closed with a solder bridge. The specimen was then subjected to a KOH etch to remove the underlying silicon substrate, leaving the thin amorphous metal attached to the copper frame closed by the solder. However, the electrodeposited copper frame had insufficient rigidity to suitable support the amorphous metal and this approach was discontinued.

The more successful approach used a copper foil window frame, cut from a thin sheet of copper (5 mil thick) and soldered carefully to the DAR 27 film. Again, the two halves of the frame were connected with a solder bridge and the silicon substrate dissolved with a alkaline etch.

For the tensile test itself, the specimen was mounted in the scanning electron microscope tensile stage, the solder bridge was carefully melted, and tensile testing of the thin film specimen was performed. However, useful data was not obtained. The surface of the DAR 27 films had degraded during the KOH etch and there were still issues with residual stress such that the film was still not perfectly flat. In each of three tests, the specimen failed prematurely as soon as loading began under essentially zero load.

Despite these disappointing results, we consider the technique developed to be essentially appropriate but issues of etching damage and alignment in the tensile stage still need to be addressed. Clearly, if deposition conditions can be modified to eliminate or reduce residual stress and if the amorphous metal were to be deposited onto a more readily dissolved substrate such as salt, then we would envisage a better result. Finally, it needs to be noted that the specimens tested were not heat treated. Heat treatment to partially devitrify the glassy metal would reduce the tendency to fail by shear banding, but we wanted to get a baseline data point on the unannealed material first.

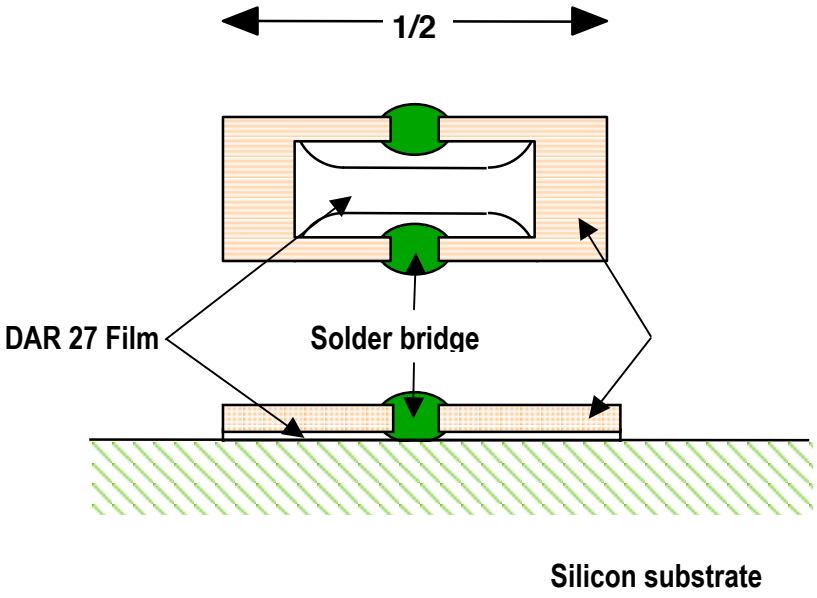

Figure 18. Schematic of tensile test specimen prior to substrate dissolution.

Ideally, tensile test structures would be fabricated by the same process used to produce the MEMS test structures. However, these small-sized tensile sample dimensions are still too large for lift-off by conventional means. The lateral etch distance required to remove the polyimide sacrificial layer would be too great.

7.0 Summary and Potential Applications

RSC and INEEL have conclusively demonstrated that amorphous metals can be patterned onto silicon substrates enabling the fabrication of MEMS devices that incorporate amorphous metals into their structure. A significant effort went into optimizing the processing conditions so that metals can be deposited as sub-micron thick, uniform, defect free coatings such that the potential performance benefit of incorporating an amorphous metal into the MEMS structure may be realized. Guckel rings, single and double ended cantilever beams and representative switch structures have all been successfully fabricated. Residual stresses and transverse stress gradients clearly exist and minimizing these stresses will be a necessary requirement if this technology is to be pursued.

It should be noted that in this Phase I effort, there was no material development. The effort addressed here used an already-developed amorphous alloy composition that shows very considerable promise as a bulk metallic glass (BMG) thick coating, where wear, hardness and adhesion are critical properties. In a subsequent effort, alloy development and optimization would be envisaged.

Characterization of the as deposited films and the test structures has used SEM, AFM, nanoindention, and tribology measurements as well as tensile testing of released films. While not all of these tests were successful, the test methodologies have been developed, if not optimized, and would be viable test methods in a Phase II effort in which a broader range of amorphous metals would be evaluated.

Since laser ablation and sputtering are viable approaches, RSC envisages teaming with a number of partners and using either thickly-coated targets or fully amorphous (bulk metallic glass) targets of various amorphous compositions in order to evaluate amorphous metals for different MEMS applications.

The amorphous metals are characterized by unique mechanical and electrochemical properties that could enable improved device-level functionality. There are a number of potential device applications that could exploit these advantages relative to traditional micromachining materials. Of the different applications that might most benefit from the incorporation of amorphous metals into MEMS devices, we have identified the following as examples of those with the potential to have high pay-off for DoD system needs:

- High flexibility, corrosion resistant membranes for pressure sensors
- Large throw actuators
- Nozzles for high pressure corrosion resistant fluids to withstand pitting and cavitation
- RF switches
- Sensors exposed to space and deep sea environments
- Resonators

The impacts of amorphous metal properties on device performance for these applications is described below:

High-Reliability Mechanical Flexures and Large Throw Actuators

MEMS devices typically incorporate elastic flexures to enable mechanical operation. For devices requiring large numbers of operations and high reliability, stable mechanical properties are required. Use of amorphous metal flexures in MEMS sensors and actuators has the potential to eliminate fatigue, and the mechanical "memory" seen in Al torsional flexures. This effect has been well documented in devices such as the TI Digital Mirror Device (DMD). The high elastic limit potential of amorphous metals would extend the range of physical displacement for compact devices. Such a development would enable applications such as high-reliability optical arrays for displays, beam steering, adaptive optics, high sensitivity strain sensors for condition based maintenance and high-g accelerometers for smart munition instrumentation. Applications to micro-valves for microfluidic systems would also benefit. Here, the large elastic displacements

would enable large deflection valve sealing mechanisms in compact device geometries, permitting higher flow rates and faster response times to be simultaneously achieved.

Hard Coatings for Micro-Nozzle Surfaces

The high hardness and excellent wear characteristics of bulk amorphous metals, if reproduced for amorphous metals at MEMS dimensions, will improve the wear performance of micro-nozzle surfaces, whether as a coating on an underlying substrate or as the structural material of the entire micro-nozzle. There is also a need to reduce pitting due to cavitation and friction effects. Such applications would exploit the extreme mechanical hardness, smooth surface, and process simplicity offered by amorphous metals and would make an attractive alternative to CVD SiC. Micronozzles are required for µturbine engines, µthrusters µchemical reactors and precision fuel injectors, for example.

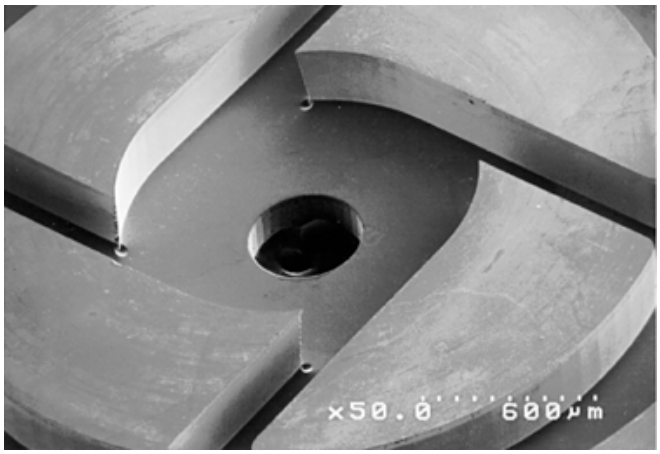

Figure 19 A Fuel Atomizer Nozzle fabricated from silicon that would be a candidate for amorphous metal material insertion.

Hard Conductive Contacts for MEMS RF Switch

MEMS RF switches represent a key technology element in the implementation of next-generation communications and radar systems. In some applications, these switch devices may need operational lifetimes in excess of 10^{12} cycles. For the case of ohmic

contact microrelays, degradation of the contact surface is a major failure mechanism that limits long-cycle operation. The successful incorporation of an amorphous metal coating on the contacting surface of a MEMS RF switch would be expected to reduce mechanical impact damage at high cycle numbers by exploiting the extreme mechanical hardness, smooth surface morphology, electrical conductivity, and the environmental stability offered by amorphous metals. Such a development would enable fabrication of e.g. phase shifters for electronically scanned antennas, tunable filters for wideband, secure communication for space-based signal routing networks. Figure 20 shows an example of an RF switch.

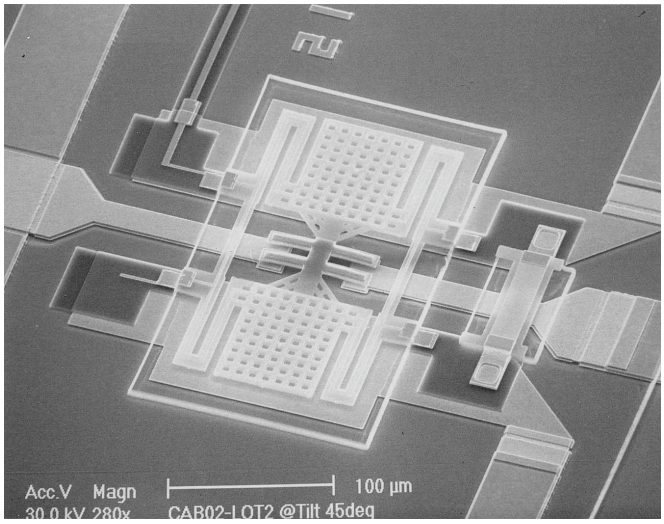

Figure 20 SEM image of MEMS RF switch

MEMS Pressure Sensor for Underwater Applications

The extreme corrosion resistance of amorphous metals would enable significant advancements in sensors for harsh environments. In particular, membrane pressure sensors for underwater applications would benefit from these properties. Presently, underwater sensors require packaging in costly and bulky stainless steel housings to provide isolation from corrosive environments. The amorphous metals could be used as the sensor's membrane diaphragm, potentially eliminating the need for secondary environmental protection. Due to the well-documented impact of packaging on device

cost (often 80%), these simplifications could translate into significant cost savings. These devices would be important for undersea applications, such as torpedo fuzing, mine and countermine devices, and underwater unmanned vehicles.

Resonators

Micromechanical resonators represent an attractive technology for timing and RF filtering applications. MEMS resonators can operate as frequency references (miniature tuning forks) or as intrinsic filter elements, coupling energy only at their mechanical resonant frequencies. These devices can enable a range of low-power, compact RF architectures. One of the key performance metrics of the resonators is their mechanical quality factor, which is related to the energy dissipation of the device. This dissipation can arise from environmental interations, substrate losses, surface losses, and internal friction. The noncrystalline internal structure of the amorphous metals may have utility in the resonator devices by reducing losses due to internal friction and hence increasing device quality factor. Attention must be paid to the other factors that contribute to the losses, however, to insure that these do not dominate the effect.